HHS Public Access

Author manuscript

*Nat Neurosci*. Author manuscript; available in PMC 2010 June 01.

Published in final edited form as:

*Nat Neurosci*. 2009 December ; 12(12): 1542–1550. doi:10.1038/nn.2442.

# Leucine-Rich Repeat Transmembrane Proteins Instruct Discrete Dendrite Targeting in an Olfactory Map

**Weizhe Hong**[1], **Haitao Zhu**[1,*], **Christopher J. Potter**[1], **Gabrielle Barsh**[1], **Mitsuhiko Kurusu**[2,3], **Kai Zinn**[2], and **Liqun Luo**[1]

[1]Howard Hughes Medical Institute and Department of Biology, Stanford University, Stanford, CA 94305, USA

[2]Division of Biology, California Institute of Technology, Pasadena, CA 91125, USA

[3]Structural Biology Center, National Institute of Genetics, and Department of Genetics, The Graduate University for Advanced Studies, Mishima 411-8540, Japan

## Abstract

Olfactory systems utilize discrete neural pathways to process and integrate odorant information. In *Drosophila*, axons of first-order olfactory receptor neurons (ORNs) and dendrites of second-order projection neurons (PNs) form class-specific synaptic connections at ~50 glomeruli. The mechanisms underlying PN dendrite targeting to distinct glomeruli in a 3-dimensional discrete neural map are unclear. Here we show that the leucine-rich repeat (LRR) transmembrane protein Capricious (Caps) is differentially expressed in different classes of PNs. Loss- and gain-of-function studies indicate that Caps instructs the segregation of Caps-positive and negative PN dendrites to discrete glomerular targets. Moreover, Caps does not mediate homophilic interactions and regulates PN dendrite targeting independent of pre-synaptic ORNs. The closely related protein Tartan plays a partially redundant function with Capricious. These LRR proteins are likely part of a combinatorial cell-surface code that instructs discrete olfactory map formation.

Spatial representation of sensory stimuli in the brain is a fundamental organizational principle that facilitates the processing and integration of sensory information[1]. In the visual and auditory systems, neurons connect nearby spatial/frequency inputs to nearby target regions in the brain, thereby forming a spatially continuous neural map. In contrast, the olfactory system utilizes discrete channels to detect olfactory information, with each channel consisting of a group of olfactory receptor neurons (ORNs) that express a specific odorant receptor. ORNs expressing the same odorant receptor converge their axons to an anatomically discrete glomerular unit in the insect antennal lobe or vertebrate olfactory bulb, the first olfactory processing center in the brain. Within each glomerulus, a single class of



Correspondence should be addressed to L.L. (lluo@stanford.edu).

*Present address: Department of Neurodegeneration, Genentech, Inc., South San Francisco, CA 94080, USA.

**Author Contributions:** W.H. performed most of the experiments and analyzed the data. H.Z. initiated the overexpression screen. C.J.P. provided unpublished *GH146*-Flp. G.B. assisted in some experiments. M.K. & K.Z. provided unpublished database and collection of fly strains for overexpression screen. W.H. & L.L. designed the experiments and wrote the paper.

ORN axons functionally synapses with the dendrites of a single class of second-order olfactory neurons: projection neurons (PNs) in insects or mitral cells in vertebrates. Thus, from insects to mammals, olfactory input and output are spatially organized into distinct channels via glomeruli, forming a discrete neural map[1]. Studies of vertebrate visual map formation have supported a crucial role for continuous gradients of guidance molecules in instructing the formation of a continuous neural map during development. However, less is known about the mechanisms by which a discrete map, exemplified by the olfactory system, is precisely constructed[1],[2].

The *Drosophila* antennal lobe consists of ~50 glomeruli, which can be uniquely identified by their stereotypical size, shape and relative position[3]. Most PNs project their dendrites to a single glomerulus and synapse with the axons of a single ORN class. The dendrite targeting of PNs to a specific glomerulus is specified by their lineage and birth order[4]. Importantly, the initial targeting of PN dendrites precedes the arrival of pioneering ORN axons[5], suggesting that the coarse glomerular map arises independently of ORN input. The *Drosophila* olfactory system thus provides an attractive model system to study mechanisms of PN dendrite and ORN axon targeting in the context of discrete map formation.

PN dendrite targeting is presumably achieved by differential expression of cell surface receptors in different classes of PNs such that they can respond differently to a common environment. Although combinatorial expression of intrinsic transcription factors in PNs has been shown to regulate PN dendrite targeting[6-8], little is known about instructive cell surface receptors during this process. The transmembrane proteins Dscam and N-Cadherin play important roles in elaboration and refinement of PN dendrites, respectively[9],[10], but they are expressed in and required for all PN classes equally. Differential expression of transmembrane Semaphorin-1a regulates coarse dendrite targeting along the dorsolateral to ventromedial axis during the initial formation of the antennal lobe[11]. However, no cell surface molecules have been shown to instruct different classes of PN dendrites to select discrete glomerular targets in a 3-dimensional neural map.

Here we report that the leucine-rich repeat transmembrane protein Capricious (Caps) is differentially expressed in different classes of PNs and cell-autonomously instructs glomerulus-specific targeting of PN dendrites. Further analysis suggests that Caps-mediated local dendrite targeting is independent of presynaptic ORNs, and does not act homophilically. We propose that Caps mediates interactions among PN dendrites, leading to a mosaic segregation of Caps-positive and negative PNs to discrete glomerular targets.

## Results

### Caps is differentially expressed in different PN classes

To identify instructive cell-surface molecules for PN dendrite targeting, we utilized a recently established database that contains 976 transmembrane and secreted molecules with potential roles in cell-cell recognition[12]. 462 transgenic lines with a UAS insertion in the 5′ end of these genes were collected that could potentially drive expression of 410 of these 976 genes, covering ~40% of the repertoire of the potential cell recognition molecules[12]. We expressed each line in a small subset of PNs using *Mz19*-Gal4[5]. We identified

P{GS6}10839 in the 5′ end of *capricious (caps)* as showing a strong PN dendrite mistargeting phenotype.

*caps* encodes a transmembrane protein with 14 leucine-rich repeats in its extracellular domain[13]. Previous studies have shown that *caps* is involved in regulating cell-cell interactions in a variety of developmental processes, including boundary formation in wing and leg discs[14],[15], organization of the morphogenetic furrow and ommatidial spacing[16], and formation of branch interconnections in tracheal development[17]. In the nervous system, *caps* has been shown to regulate the axon targeting of motor neurons to specific subsets of muscles[12],[13] and axon targeting of R8 photoreceptor neurons to the proper layer in the medulla[18].

Staining with polyclonal antibodies against Caps shows that Caps protein is present in the developing antennal lobe (Fig. 1a-f; Fig. S1). Around 48 hrs after puparium formation (APF) when individual glomeruli in the antennal lobe are just becoming identifiable, differential Caps expression is evident with high levels in some glomeruli and low or undetectable levels in others (Fig. 1b and 1e). The distinct expression levels of Caps do not arise from a differential density of neurites, since the density of neurites is rather uniform between different glomeruli as shown by staining of nc82, a pre-synaptic marker[19] (Fig. 1a and 1d). The Caps staining is eliminated in a loss-of-function *caps* mutant (Fig. 1h), indicating that the antibody is specific to endogenous Caps protein. Furthermore, the expression of UAS-mCD8GFP driven by the enhancer trap *caps*-Gal4 recapitulates the glomerular-specific anti-Caps staining pattern (Fig. 1c and 1f, compared with Fig. 1b and 1e), suggesting that *caps*-Gal4 is a faithful reporter of endogenous Caps expression.

At 48 hrs APF, the antennal lobe consists of dendrites from PNs and axons from ORNs. To determine the contribution to *caps* expression by PN dendrites, we generated a PN-specific flipase line *GH146*-Flp. Similar to the *GH146*-Gal4 expression pattern, *GH146*-Flp is expressed in the majority of PNs; these PNs innervate 40 out of the 46 glomeruli scored (Fig. S2a). Therefore, we used a Flp-out GFP reporter *UAS>stop>mCD8GFP* to determine the intersection of *GH146*-Flp and *caps*-Gal4, and thus Caps expression in PNs (Fig. S2b). Interestingly, *caps*-Gal4 is selectively expressed in a subset of PNs innervating 23 out of 40 *GH146*-positive glomeruli (Fig. 1i-l, Fig. S2b). Glomerular targets of Caps-positive and Caps-negative PNs do not segregate into broad domains, and appear intercalated (Fig. 1l).

## Loss of *caps* causes mistargeting in Caps-positive PNs

The differential expression of Caps in different glomeruli raised the possibility that Caps instructs targeting of PN dendrites to specific glomeruli according to Caps expression patterns. This hypothesis predicts that loss of Caps in Caps-positive PNs should cause their dendrites to mistarget to glomeruli normally innervated by Caps-negative PNs, whereas it may not affect the dendrite targeting of Caps-negative PNs. We first tested this prediction by performing loss-of-function MARCM analyses using the null allele $caps^{c28fs}$ for the lateral neuroblast clone containing 12 classes of PNs, 9 of which are Caps-positive. Loss of *caps* in the lateral neuroblast clones results in two types of dendrite targeting defects: loss of innervation in glomeruli that are normally targets of lateral PNs, and gain of innervation in glomeruli that are normally not the targets of lateral PNs (Fig. 2a-c). In accordance with our

prediction, quantitative analysis of dendrite distribution in *caps* mutants shows that all the glomeruli that exhibit loss of innervation are targets of Caps-positive PNs, whereas the ectopically innervated glomeruli are mostly normal targets of Caps-negative PNs (Fig. 2d). This bias of mistargeting towards normal Caps-negative PN targets is highly significant ($X^2$, $p<0.001$; Fig. S3a). Notably, loss of *caps* in Caps-positive PNs does not cause a random mistargeting of dendrites to all Caps-negative targets but a preferential mistargeting to specific ectopic targets (Fig. 2d).

The analysis of 12 PN classes in neuroblast clones suggests that *caps* is required in PNs for proper dendrite targeting. However, it is difficult to determine exactly which classes of PNs contribute to the ectopic innervations and whether the loss of innervation is caused by mistargeting rather than gross defects in dendrite arborization. In addition, it is unclear whether the phenotype is caused by a cell-autonomous requirement for *caps*. To address these questions, we performed MARCM analysis of specific PN classes, including single cell clones. Using *GH146*-Gal4 and *MZ19*-Gal4, along with additional information of neuroblast lineage, heat shock window, and axon branching pattern, we sampled four Caps-negative (DL1, DA1, DC3, and VA1d) and four Caps-positive (VC1, VC2, VA4, and DM1) PN classes innervating different regions in the antennal lobe (see Methods).

Consistent with our prediction, the four Caps-negative PN classes (DL1, DA1, DC3, and VA1d) do not exhibit detectable dendrite targeting defects (Fig. 3, a-c and h-j). However, loss of *caps* in four Caps-positive PN classes (VC1, VC2, VA4, and DM1) results in innervation of additional ectopic glomeruli normally targeted by Caps-negative PNs (Fig. 3, d-g, k-n). All $caps^{-/-}$ VC1 PNs exhibit strong ectopic innervation, and 92% of this ectopic innervation occurs in the DA2, DC2, VM7, DC1 and VM5 glomeruli, all of which are normally innervated by Caps-negative PNs (Fig. 3s-t). Similarly, loss of *caps* in the Caps-positive VC2, VA4 and DM1 PNs results in strong ectopic innervation of the VM7, DA2 and VM5 glomeruli, all of which are normally innervated by Caps-negative PNs (Fig. 3u-v). In both cases, the bias of mistargeting towards normal caps-negative PN targets is highly significant ($X^2$, $p<0.01$; Fig. S3b, c). Therefore, the loss-of-function analysis in both neuroblast and single cell clones suggests that Caps instructs the segregation of Caps-positive and negative PN dendrites to different glomeruli. In the absence of Caps, Caps-positive PNs retain part of their dendrites in their normal glomeruli, but mistarget part of their dendrites preferentially into glomeruli that are normal targets of Caps-negative PNs. We further noticed that the ectopic glomeruli mistargeted by $caps^{-/-}$ PNs tend to be in close proximity to their normal glomerular targets (e.g. Fig. 3w for VC1), suggesting that Caps regulates local dendrite targeting.

To test the cell-autonomy of Caps function, we used MARCM to express a UAS-*caps* transgene only in single cells that are homozygous mutant for *caps* and labeled by mCD8-GFP. This results in a rescue of the dendrite mistargeting phenotype of all four Caps-positive PNs (Fig. 3o-r, s, u). Since the *GH146*-Gal4 used for rescue is expressed only in postmitotic PNs[8], the rescue experiment demonstrates that Caps is cell-autonomously required in postmitotic neurons for the dendrite targeting of these Caps-positive PNs.

In contrast to dendrite mistargeting, lateral horn axon terminal arborization patterns of *caps* mutant PNs still follow their class-specificity previously described[20-22] (Fig. S4, see Methods). This suggests that *caps* regulates targeting of dendrites as opposed to general fate determination of PNs, and that dendrite targeting and axon terminal arborization are separable processes.

## Misexpression causes mistargeting in Caps-negative PNs

We have shown that loss of Caps in Caps-positive PNs causes dendrite mistargeting preferentially to glomerular targets of Caps-negative PNs. Next, we tested whether ectopic expression of Caps in Caps-negative PNs would cause dendrite mistargeting, and whether such mistargeting would be preferential to glomeruli that are normally innervated by Caps-positive PNs. We found that MARCM overexpression of Caps in PN neuroblast clones caused severe mistargeting, resulting in a deformation of the entire antennal lobe structure (Fig. 4a-d). Next, we misexpressed Caps using *Mz19*-Gal4 in 3 classes of PNs, DA1, VA1d and DC3, which are all Caps-negative and send their dendrites to 3 adjacent glomeruli (Fig. 4e-f). Caps misexpression by *Mz19*-Gal4 shows a mistargeting of dendrites to nearby VA1lm (81%) and VA4 (31%), both of which are targets of Caps-positive PNs (Fig. 4f, arrowheads).

We further misexpressed Caps in a single DL1 PN, which normally neither expresses Caps (Fig. 1l) nor requires Caps for targeting (Fig. 3h). Caps misexpression produces partial loss of innervation of the DL1 glomerulus and ectopic innervation of a selective subset of other glomeruli (Fig. 4g-i); these ectopic glomerular targets are normally innervated by Caps-positive PNs except DP1l whose Caps expression status is undetermined (Fig. 4j). This bias of mistargeting towards normal caps-positive PN targets is highly significant ($X^2$, $p<0.001$; Fig. S3d), supporting the hypothesis that Caps instructs PN dendrite targeting by segregating Caps-positive and negative PNs. Notably, over 2/3 of the mistargeting events occur at glomeruli near DL1 (DL2d, DL2v, VL2a and VL2p) (Fig. 4k), suggesting that mistargeting is preferentially local. We also noticed that mistargeted dendrites avoid two glomeruli DL4 and DL5, which are adjacent to DL1 and innervated by Caps-positive PNs (Fig. 4k), suggesting that mistargeting is not random among local ectopic targets (see Discussion).

Caps misexpression in single DL1 PNs does not affect PN axon targeting in the lateral horn (Fig. S4c), further confirming that *caps* specifically regulates the specificity of dendrite targeting as opposed to the general determination of cell fate.

## *caps* is not required for ORN axon targeting

The expression pattern, loss- and gain-of-function data presented so far demonstrate that Caps instructs targeting of PN dendrites by segregating Caps-positive and negative PNs to discrete glomerular targets. We next explored the cellular mechanisms by which Caps functions to regulate dendrite targeting. Caps has been proposed to determine axon-target connectivity by regulating the interaction between photoreceptor or motor axons and their postsynaptic targets[13,18]. This model is further supported by a recent observation that Caps appears to mediate direct interaction between postsynaptic filopodia of muscles and presynaptic growth cones[23].

PNs send their dendrites to the developing antennal lobe prior to the arrival of pioneering ORN axons[5]. The dendrites subsequently elaborate and refine their processes while ORNs extend their axons into the antennal lobe[9], [10]. The glomerular positionings of dendrites and axons eventually require pre- and postsynaptic interactions, to achieve the proper matching specificity between PNs and ORNs[9]. If Caps has an analogous function in the olfactory system as in motor neurons and photoreceptors, it might mediate interactions between ORN axons and PN dendrites. However, the following experiments strongly argue against this model.

To determine whether *caps* is also expressed in presynaptic ORNs, we examined the expression intersection between *caps*-Gal4 and *ey*-Flp. *ey*-Flp is expressed in precursors of ORNs but not in central neurons including PNs[24], thereby allowing us to specifically visualize *caps*-Gal4 expression in ORNs using a Flp-out reporter. We found that *caps*-Gal4 is expressed in a subset of ORNs selectively innervating 28 out of 46 glomeruli (Fig. 5a-d, Fig. S2c). However, glomeruli innervated by Caps-expressing PNs and ORNs exhibit only partial overlap (Fig. 5e, Fig. S2c), and the correlation between Caps expression in PNs and ORNs is not statistically significant ($X^2$, $p>0.3$).

To test whether *caps* is required in ORNs for their axon targeting, we removed *caps* from about half of ORNs using the *ey*-Flp MARCM strategy[24] and analyzed targeting of 9 different ORN classes using Or-Gal4 or AM29-Gal4 lines to label specific classes of ORN axons. These 9 classes of ORN-PN pairs sample 4 pairs of Caps-positive ORNs and Caps-positive PNs (Or22a - DM2, Or47a - DM3, Or47b - VA1lm, AM29 - DM6), 4 pairs of Caps-positive ORNs and Caps-negative PNs, (Or46a - VA7l, Or59c - VM7, Or67b - VA3, Or88a - VA1d) and 1 pair of Caps-negative ORNs and Caps-positive PNs (AM29 - DL4). None of these 9 ORN classes exhibit any obvious axon targeting defects (Fig. 5f-i; data not shown), indicating that *caps* is not cell-autonomously required in ORNs for their proper axon targeting.

In addition, when glomerular position of PN dendrites is shifted as a result of loss of *caps* in ventral VA1lm PNs, the axons of presynaptic Or47b ORNs shift accordingly without compromising the matching between ORN axons and PN dendrites (Fig. S5). Thus, loss of Caps in PNs does not appear to disrupt the proper targeting of ORN axons, at least for the specific ORN-PN pair we tested.

## Caps-mediated PN dendrite targeting is independent of ORNs

Even though Caps is not required for ORN axon targeting, Caps-dependent PN dendrite targeting could in principle still depend on the interaction with cues from ORNs. Two lines of evidence already argue against the possibility that Caps itself provides the putative ORN derived cue. First, there is only partial overlap between Caps expression pattern in PNs and ORNs (Fig. 5e, Figure S2). Second, both loss of innervation and ectopic innervation of PN dendrites occur in glomerular targets of both Caps-positive and Caps-negative ORNs with no obvious preference (Figure S3a-d). These observations argue against a specific hypothesis that PN dendrite targeting is dependent on homophilic interactions of Caps between PN dendrites and ORN axons. Below we provide two lines of evidence further suggesting that Caps-mediated PN dendrite targeting is independent of ORN axons.

We have previously shown that PNs start to elaborate dendrites shortly after puparium formation and that PN dendrites localize to their initial stereotypical target region of the developing antennal lobe before pioneering ORN axons arrive at 18 hrs APF[5]. Therefore, an examination of dendrites at 16 hrs APF will allow us to examine the ORN-independent phase of early PN dendrite targeting. Developmental time course analysis of Caps expression in the antennal lobe indicates that at 12-16 hrs APF, the developing antennal lobe is already stained positive for both Caps-specific antibody and *caps*-Gal4 expression (Fig. S1), confirming that Caps is expressed in developing PN dendrites. At 16 hrs APF, all wild-type DL1 PN dendrites localize to the dorsal-lateral corner of the developing antennal lobe (Fig. 6a); however, Caps misexpression in DL1 already causes dendrites to extend across the midline of the dorsomedial-ventrolateral axis of the antennal lobe in ∼40% of the samples (Fig. 6b), arguing against the possibility that Caps mediates interactions between PN dendrites and ORN axons, at least for PN initial targeting. The medial mistargeting phenotype persists at 48 hrs APF (Fig. 6d, compared with Fig. 6c), and the penetrance of mistargeting is comparable among different developmental stages (Fig. 6e), suggesting that adult defects are likely caused by defects in early PN dendrite targeting.

To further test whether ORN axons are involved in Caps-instructed PN dendrite targeting at a later developmental stage, we compared Caps misexpression phenotypes in an otherwise normal or ORN-ablated background. If Caps instructs PN dendrite targeting by mediating the interactions between ORN axons and PN dendrites, we expect that ORN ablation would suppress the mistargeting phenotypes of PN dendrites caused by PN misexpression of Caps. To ablate all ORNs during early development, we used *Pebbled*-Gal4 and *ey*-Flp to express the flip-out toxin *UAS>stop>RicinA. Pebbled*-Gal4 and *ey*-Flp are expressed in all ORNs during early development[24] and therefore this strategy ablates almost all ORNs before their axons enter the developing antennal lobe (Fig. S6). *ey*-Flp is not expressed in PNs or their progenitors, allowing us to simultaneously use a PN-specific *Mz19*-Gal4 line to assess PN dendrite development in ORN ablated animals.

*Mz19*-Gal4 labels 3 PN classes innervating 3 adjacent glomeruli, DA1, VA1d and DC3, located in the dorsolateral region of the antennal lobe (Fig. 6f). When ORNs are ablated during development, the dendrites of these 3 PN classes still converge to discrete regions and remain adjacent to each other, although they are located in the ventrolateral region due to a shift of the antennal lobe orientation in the absence of ORN axons (Fig. 6h). The ablation experiment suggests that PNs retain their intrinsic ability to converge their dendrites to specific glomerular regions at both early and later developmental stages without the contribution of ORN axons. Caps misexpression by *Mz19*-Gal4 results in mistargeting of PN dendrites to VA1lm and VA4 and the dendrites were frequently segregated to non-adjacent regions in the antennal lobe as a consequence of this mistargeting (Fig. 6g). Interestingly, this dendrite segregation also occurred when Caps is misexpressed by *Mz19*-Gal4 after ablating all ORNs (Fig. 6i), and the penetrance is comparable to Caps misexpression without ORN ablation (Fig. 6j).

Taken together, these data strongly suggest that Caps instructs PN dendrite targeting independently of ORN axons throughout development. Besides ORNs, PNs are the only cell type that can provide class-specific positional cues. Given the mosaic distribution of Caps-

positive and negative glomeruli, we suggest that Caps regulates PN dendrite targeting through PN-PN interactions—as opposed to responding to a global cue—leading to a segregation of Caps-positive and negative PNs (see Discussion).

## Caps does not mediates homophilic interactions

Caps has been proposed to act as a homophilic recognition molecule based on its ability to promote S2 cell aggregation, although this can only be seen when the expression level is very high[13,14,18] (A. Nose, personal communication). Here, we used a genetic approach to functionally test whether Caps mediates homophilic interactions *in vivo* during PN dendrite targeting. We have shown that Caps misexpression in a single Caps-negative DL1 PN results in a preferential mistargeting (Fig. 4h-i and 7b). If homophilic interactions among Caps-expressing cells underlie this misexpression phenotype, we would expect that eliminating endogenous Caps expression in the entire animal would suppress this phenotype.

The *caps* homozygous mutants die primarily as embryos, but a few escapers (<0.1%) survive until adulthood. DL1 PN dendrites still target properly to the DL1 glomerulus in these *caps* homozygous mutant escapers (Fig. 7a). However, ectopic expression of Caps in a single DL1 PN in these *caps* mutant escapers still caused mistargeting of DL1 dendrites to ectopic glomeruli in the antennal lobe (Fig. 7c). Quantification shows that Caps misexpression in single DL1 PN caused a similar degree of mistargeting in a whole animal $caps^{-/-}$ background as in the wild type (Fig. 7d), indicating that Caps-dependent dendrite targeting does not use Caps in other cells as a cue, at least in the gain-of-function context. Overall, these data suggest that Caps uses a heterophilic ligand to instruct dendrite targeting.

## Partially redundant function of Caps and Trn

Caps shares 67% sequence identity in its extracellular domain with another leucine-rich repeat transmembrane protein Tartan (Trn)[13,25], the closely related paralog of Caps. *trn* and *caps* have redundant functions in regulating boundary formation in wing imaginal dics[14,26], leg segmentation[15], and the architecture of the morphogenetic furrow and ommatidial spacing[16]. In the nervous system, *trn* and *caps* also have redundant functions in regulating motor axon targeting[12,23]. Indeed, Trn overexpression also results in dendrite mistargeting phenotypes in neuroblast and DL1 single PN clones (Fig. S7a-f). Moreover, expression of an enhancer trap *trn*-lacZ together with *caps*-Gal4, *GH146*-Flp and *UAS>stop>mCD8GFP* suggests that *trn* is expressed in PNs and partially overlaps with *caps* expression (Fig. S7g).

To test the requirement of *trn* in PN dendrite targeting, and its potential redundant function with Caps, we performed loss-of-function studies of *trn* single and *trn caps* double mutants analogous to the *caps* studies described above (Fig. 8). We found that loss of *trn* in the lateral neuroblast clone resulted only in ectopic innervation, but two independent *trn caps* double mutant pairs showed a significantly higher percentage of combined loss-of-innervation and ectopic innervation compared with either of the single mutants (Fig. 8a). A glomerulus is usually innervated by multiple PNs so that ectopic innervation reflects a partial mistargeting of these PNs whereas loss-of-innervation indicates all these PNs completely mistarget away from the normal region. The loss-of-innervation of VA7m, VC1 and VC2 were not observed in either *caps* (Fig. 2d) or *trn* single mutants but occurred

frequently in *trn caps* double mutants (Fig. 8c), indicating that *trn caps* double mutants exhibit more severe mistargeting phenotypes. Furthermore, single cell loss-of-function analysis of VC1 and VC2/VA4/DM1 PNs consistently exhibited more severe mistargeting phenotypes for double mutants than either of the single mutants (Fig. 8b). For example, *caps* single mutant VC1 PNs always retain a part of their dendrites in the VC1 glomerulus (Fig. 8b, e); however, a large percentage of *trn caps* double mutant VC1 PNs no longer innervate VC1 at all (Fig. 8b, g, h), consistent with the strong loss-of-innervation of VC1 observed in lateral neuroblast clones of *trn caps* double mutants. However, similar to the *caps* single mutant, neither *trn* single nor *trn caps* double mutants exhibit any detectable targeting defects in the axons of 9 different ORN classes tested for *caps* single mutants (data not shown), suggesting that Trn and Caps are dispensable for ORN axon targeting.

Given that Caps and Trn have high sequence similarity, similar overexpression phenotypes, overlapping expression patterns, and enhancement of PN dendrite mistargeting in double mutants compared with either of the single mutants alone, we conclude that Caps and Trn play partially redundant function in PN dendrite targeting.

## Discussion

### Discrete cell surface codes in a discrete neural map

Graded expression of guidance molecules is widely used in patterning continuous, topographic representation of sensory inputs. A classic example is graded Ephrin/Eph signaling in regulating retinotopic projections in vertebrates[1,27]. Graded molecules may also be used in the initial coarse patterning of discrete olfactory maps in flies and mice[11,28], but selective targeting to discrete glomerular units requires additional mechanisms. Here, we showed that the LRR transmembrane protein Caps is expressed in a subset of PNs whose dendrites target to a subset of glomeruli intermingled with other glomeruli targeted by Caps-negative PNs. Loss of *caps* selectively affects targeting of Caps-positive PNs, causing them to partially but preferentially mistarget to glomeruli normally innervated by Caps-negative PNs. Conversely, misexpression of Caps in Caps-negative PNs causes them to selectively target dendrites to glomeruli that are normal targets of Caps-positive PNs. These data demonstrate that Caps instructs the segregation of Caps-positive and negative PN dendrites to discrete glomerular targets in the *Drosophila* antennal lobe.

How does Caps-mediated targeting act together with molecular gradients used for establishing the coarse dendrite map? A general conceptual problem of making a discrete map based on gradient cues is that nearby discrete glomerular units have to be distinguished with a minimal difference in gradient cues. One potential solution would be to set a second type of cell surface molecules that form a spatially intercalated expression pattern with a tight correlation with each discrete class of neurons. Indeed, recent studies in mouse ORN axon targeting suggested a hierarchical model in which molecular gradients help coarse targeting of axons, followed by local refinement mediated by activity-dependent expression of cell recognition molecules[1,2]. Neuropilin-1 and Semaphorin-3A are expressed in broad domains in olfactory bulb and disruption of Semaphorin-3A causes global axon mistargeting[29-33]. However, other cell surface molecules, including Ephrin-A2/A5 and EphA5, as well as immunoglobulin superfamily proteins Kirrel-2, Kirrel-3, and BIG-2, are

differentially expressed in a mosaic pattern and likely regulate local axon targeting through axon-axon interactions among ORNs[34-36].

*Drosophila* PN dendrite targeting appears to utilize a conceptually similar strategy even though details may differ regarding types of molecules, cells (ORNs vs. PNs), neuronal processes (axons vs. dendrites), and dependence on activity; this hierarchical regulation may be a general strategy for discrete map formation. Specifically, we propose that molecular gradients such as Semaphorin-1a may set up a coarse map for PN dendrites. This is followed by Caps-dependent local dendrite targeting to discrete glomeruli. In support of this notion, loss of *semaphorin-1a* causes a directional shift of dendrites[11], whereas loss of *caps* cause a specific mistargeting to local ectopic targets.

Both loss-of-function and misexpression analyses indicate that the mistargeted dendrites are restricted to only a subset of ectopic glomeruli following the Caps code. For example, Caps-misexpressing DL1 PNs mistarget to the DL2v and DL2d glomeruli but avoid DL4 and DL5 glomeruli, even though they are all in the vicinity of DL1 and are normal targets of Caps-positive PNs. Similarly, *caps* loss-of-function in VC1 PNs causes dendrites to mistarget to VM7, DC2, DC1, VM5 but avoid VL1, DP1m and DC3, even though they are all in the vicinity of VC1 and are normal targets of Caps-negative PNs. These observations suggest that additional molecules must work together with Caps to distinguish targeting specificity among different Caps-positive PNs or among different Caps-negative PNs. Since these additional molecules are still intact in PNs with an altered Caps code, their actions might explain the mistargeting specificity. Thus, Caps likely acts in parallel with additional molecules to specify dendrite targeting of the 50 PN classes into areas that eventually develop into 50 glomeruli.

## Cellular and molecular mechanisms

The matching expression of Caps in motor neurons and their target muscles[12,13], as well as in R8 photoreceptor axons and their target layers[18], suggest that Caps functions in synaptic matching through interactions between pre- and post-synaptic partners. During the assembly of the olfactory system, 50 classes of ORN axons need to match with 50 classes of PNs. However our data strongly argue against the possibility that the PN dendrite targeting defect is caused by a predominant role of Caps in mediating synaptic matching between ORN axons and PN dendrites. First, *caps* is required for targeting of PN dendrites but not ORN axons. This cannot be caused by the redundancy with a close paralog Trn, as *trn caps* double mutants enhance *caps* phenotypes in PN dendrite targeting, but still exhibit no phenotypes in ORNs. Second, expression patterns of Caps in PNs and ORNs do not match with regard to their glomerular targets. Third, Caps-mediated PN dendrite targeting is independent of ORNs. Fourth, Caps misexpression phenotype is not affected by the loss of Caps in all other cells, suggesting that it interacts with a heterophilic ligand for PN dendrite targeting.

The use of a heterophilic ligand is consistent with studies of Caps in boundary formation of the wing imaginal disc[14,26]. Given the mosaic distribution of Caps-positive and negative glomeruli, as well as the analogy with the axon-axon interactions in refining local targeting of mouse ORN axons, we propose that the heterophilic Caps ligand is most likely derived

from other PNs, and that the interactions between Caps and its ligand mediate PN-PN interactions to segregate Caps-positive and negative PNs to specific glomeruli.

How do Caps and its heterophilic ligand segregate Caps-positive and negative PNs via PN-PN interactions? The simplest hypothesis consistent with our data is that a repulsive ligand is expressed in Caps-negative PNs, forming a mosaic pattern complementary to Caps. Caps and its ligand mediate repulsive interactions among PN dendrites to segregate Caps-positive and negative PNs. When Caps is lost in a Caps-positive PN, its dendrites innervate ectopic glomeruli that are preferentially targets of Caps-negative PNs because of a loss of repulsion from Caps-negative PN dendrites; additional molecules that normally instruct Caps-positive PN dendrites to select a specific Caps-positive glomeruli are still intact, thereby preventing *caps* mutant PNs from invading other Caps-positive glomeruli. When Caps is misexpressed in a Caps-negative PNs, the repulsive ligand would force dendrites to mistarget to glomerular targets of Caps-positive PNs. Future identification of the Caps ligand will be essential to test this hypothesis, and will shed further light on the mechanisms of discrete olfactory map formation.

## Methods

### Fly stocks

*GH146*-Gal4[37] and *Mz19*-Gal4[5] are used to label PNs. Or-Gal4 lines (Or22a-Gal4, Or46a-Gal4, Or47a-Gal4, Or47b-Gal4, Or59c-Gal4, Or67b-Gal4, Or88a-Gal4)[24,38-41] and AM29-Gal4[42] are used to label ORNs. The enhancer trap line *caps*-Gal4 (NP3294)[18] is used to visualize Caps-expressing neurons and *trn-lacZ*[25] is used to visualize Trn-expressing cells. P{GS6}10839 (*caps*) and P{GS6}10885 (*trn*) were generated by *Drosophila* Gene Search Project (Metropolitan University, Tokyo)[43]. The single and double null mutant alleles of *caps* and *trn* used are $caps^{c28fs}$ *FRT2A*[15,18], $trn^{28.4}$ *FRT2A*[15,25], $trn^{\Delta 17}$ $caps^{c28fs}$ *FRT2A*[15], *and* $trn^{28.4}$ $caps^{\Delta 1}$ *FRT80B*[16] as well as a small *caps* deficiency allele *Df(3L)Ex6118*. $caps^{c28fs}$ contains a 7-base pair deletion, which results in a frame shift after the first 28 amino acids[15,18]. $trn^{28.4}$ carries a small deletion of *trn* gene generated by P-element excision[25]. $trn^{\Delta 17}$ $caps^{c28fs}$ was generated based on the null allele $caps^{c28fs}$ and carries an additional deletion covering the entire *trn* coding sequence[15]. $trn^{28.4}$ $caps^{\Delta 1}$ was generated based on the null allele $trn^{28.4}$, and carries an additional deletion covering the entire *caps* coding sequence[16]. UAS-*caps* transgene[13] inserted on the 3rd chromosome is used for rescue and misexpression experiments. Flies used in the overexpression screen were previously described[12].

### Clonal analysis

The MARCM method was applied as described previously[44,45]. Briefly, *caps* and/or *trn* alleles were placed transheterozygous to Gal80 on the FRT chromosome arm[15,18]. Flipase activity causes mitotic recombination of the FRT chromosome arm such that one of the daughter cells become homozygous for *caps* or *trn* and simultaneously loses Gal80. This cell (and its progeny) can therefore be labeled by the Gal4/UAS system.

For ORN analysis, *eyFlp* was utilized to induce clones in nearly half of the ORNs and Or-specific Gal4 lines were used to label these clones.

For PN analysis, clones were generated by *hsFlp* and labeled by *GH146*-Gal4 or *Mz19*-Gal4. For generating neuroblast clones, flies were heat-shocked between 24–36 hrs after egg laying for 1 hr at 37 °C. For generating class-specific clones, flies were heat-shocked during a unique time window after egg laying (AEL) for 1 hr at 37 °C and the clone identities were determined by a combined information of Gal4 lines used, heat shock window, neuroblast lineage, and axon branching pattern. Four Caps-negative (DL1, DA1, DC3, and VA1d) and four Caps-positive (VC1, VC2, VA4 and DM1) PN classes are investigated here. *Mz19*-Gal4 labels DC3 and VA1d from the anterodorsal neuroblast and DA1 from the lateral neuroblast[5]. We used *MZ19*-Gal4 to analyze dendrite targeting of DC3/VA1d and DA1 by generating neuroblast clones at 24–36 hrs AEL. The other five classes were analyzed as single cell clones using *GH146*-Gal4. To analyze DL1 PNs, we heat-shocked flies between 24–36 hrs AEL—100% anterodorsal PN single cell clones generated at this time are DL1[4]. To analyze the four Caps-positive PNs in the lateral lineage, we identified a time window of clone induction (36-48 hrs AEL) in which all *GH146*-Gal4-positive single cell PN clones generated from the lateral neuroblast are *caps*-positive and project their dendrites to VA4, DM1, VC1 or VC2 glomerulus in wild-type controls (Fig. 3d-g). The axon branching pattern of VC1 in the lateral horn is uniquely identifiable among the four groups and is unchanged in *caps* mutants (Fig. S4). (We performed a blind test of mixing axon patterns of single cell MARCM clones of 4 PN classes each with 3 genotypes—control, mutant and rescue, and all VC1 PNs were identified in the blind test with 100% accuracy; the mutant VC1 samples were additionally validated by their partial dendrite innervation of VC1 in additional to ectopic glomeruli.) These criteria allowed us to identify VC1 PNs unequivocally. The other three Caps-positive PN classes (VC2, VA4 and DM1) also have characteristic lateral horn axon branching patterns that are largely unchanged in mutants. However their axon branching patterns are more similar to each other and were not 100% identified in our blind test. Therefore we analyzed dendrite mistargeting of these three classes together (Fig. 3u-v). We assigned a class to each representative image in Fig. 3l-n based on their partial innervation of VC2, VA4 or DM1. Animals were raised at 25 °C after heat-shock and dissected 5–7 days after eclosion.

For analyzing DL1 single cell misexpression during development, flies were raised at 29 °C after heat-shock to increase expression level and overcome Gal80 perdurance. Animals were dissected at 12 hrs APF and 36 hrs APF at 29 °C, which are equivalent to 16 hrs APF and 48 hrs APF at 25 °C, respectively.

To determine whether the preference of mistargeting events that occur in glomerular targets of Caps-positive or negative PNs (or ORNs) is statistically significant, each experiment was tested by $X^2$ based on the null hypothesis that mistargeting events occur randomly in Caps-positive and negative glomeruli. p values were shown for each experiment and used to accept or reject the null hypothesis.

Genotypes for PN MARCM analysis: *hsFlp$^{122}$ UAS-mCD8GFP; GH146-Gal4 UAS-mCD8GFP; caps (and/or trn) FRT2A (or FRT80B) / G80 FRT2A (or FRT80B).* For ORN

analysis: *eyFlp UAS-mCD8GFP; Or-Gal4 UAS-mCD8GFP; caps (and/or trn) FRT2A/G80 FRT2A*.

### New transgenes

*GH146*-Flp cloning: The p[GAL4, w+]$^{GH146}$ enhancer trap is inserted in the 5′ upstream region of the *oaz* gene (*CG17390*). The cloned *GH146* genomic enhancer is a 12.6 kB fragment that includes all genomic DNA between oaz and the upstream gene *CG17389* as well as all *oaz* introns. The GAL4 coding region from pBAC-3xPDsRed-GH146-GAL4[46] was replaced with GAL80 to generate pBAC-3xPDsRed-GH146-GAL80 (Potter and Luo, unpublished). Site-directed mutagenesis of pBAC-3xPDsRed-GH146-GAL80 was used to introduce FseI and AvrII restriction sites flanking the GAL80 coding region. A linker oligo was ligated into the FseI/AvrII site to generate pBAC-3xPDsRed-GH146-MCS with multicloning site FseI-AscI-AvrII. Mammalian optimized FLPase (FLPo; Addgene plasmid 13792)[47] was PCR amplified to include FseI/AvrII restriction sites, and cloned into pBAC-3xPDsRed-GH146-MCS to generate pBAC-3xPDsRed-GH146-FLPo.

UAS-FRT-Stop-FRT-mCD8GFP cloning: The FRT-stop-FRT cassette, with additional BglII/NotI restriction sites, was PCR amplified from genomic DNA of UAS-FRT-stop-FRT-shibire$^{ts}$ flies[48] and cloned into pUAST-mCD8GFP[45] to generate pUAST-FRT-stop-FRT-mCD8GFP. All constructs were sequence verified. Transgenic animals were generated as previously described[49].

### Immunochemistry

The procedures for fixation, immunochemistry and imaging were as described previously[50]. Primary antibodies are Mouse nc82 (1:30), Rat anti-N-cadherin (1:40), Rat anti-mCD8 (1:100), Chicken anti-GFP (1:300) and Rabbit anti-Caps (1:100)[13].

## Supplementary Material

Refer to Web version on PubMed Central for supplementary material.

## Acknowledgments

We thank A. Nose (University of Tokyo, Japan), S. Cohen (Temasek Life Sciences Laboratory, Singapore), M. Freeman (MRC Laboratory of Molecular Biology, UK), S. Hayashi (Riken Center for Developmental Biology, Japan), and M. Milan (Icrea and Parc Cientific de Barcelona, Spain) for fly stocks and reagents; Bloomington, Szeged, Kyoto, and Harvard Stock Centers for fly stocks; M. Spletter for making antennal lobe schemes, T. Clandinin, K. Miyamichi, M. Spletter, L. Sweeney, J. Wu, X. Yu, D. Berdink, and other lab members for comments and discussions. This work was supported by NIH grant R01-DC005982. L.L. is an investigator of the Howard Hughes Medical Institute.

## References

1. Luo L, Flanagan JG. Development of continuous and discrete neural maps. Neuron. 2007; 56:284–300. [PubMed: 17964246]
2. Imai T, Sakano H. Roles of odorant receptors in projecting axons in the mouse olfactory system. Curr Opin Neurobiol. 2007; 17:507–515. [PubMed: 17935969]
3. Laissue PP, et al. Three-dimensional reconstruction of the antennal lobe in Drosophila melanogaster. J Comp Neurol. 1999; 405:543–552. [PubMed: 10098944]

4. Jefferis GS, Marin EC, Stocker RF, Luo L. Target neuron prespecification in the olfactory map of Drosophila. Nature. 2001; 414:204–208. [PubMed: 11719930]
5. Jefferis GS, et al. Developmental origin of wiring specificity in the olfactory system of Drosophila. Development. 2004; 131:117–130. [PubMed: 14645123]
6. Komiyama T, Johnson WA, Luo L, Jefferis GS. From lineage to wiring specificity. POU domain transcription factors control precise connections of Drosophila olfactory projection neurons. Cell. 2003; 112:157–167. [PubMed: 12553905]
7. Komiyama T, Luo L. Intrinsic control of precise dendritic targeting by an ensemble of transcription factors. Curr Biol. 2007; 17:278–285. [PubMed: 17276922]
8. Spletter ML, et al. Lola regulates Drosophila olfactory projection neuron identity and targeting specificity. Neural Dev. 2007; 2:14. [PubMed: 17634136]
9. Zhu H, et al. Dendritic patterning by Dscam and synaptic partner matching in the Drosophila antennal lobe. Nat Neurosci. 2006; 9:349–355. [PubMed: 16474389]
10. Zhu H, Luo L. Diverse functions of N-cadherin in dendritic and axonal terminal arborization of olfactory projection neurons. Neuron. 2004; 42:63–75. [PubMed: 15066265]
11. Komiyama T, Sweeney LB, Schuldiner O, Garcia KC, Luo L. Graded expression of semaphorin-1a cell-autonomously directs dendritic targeting of olfactory projection neurons. Cell. 2007; 128:399–410. [PubMed: 17254975]
12. Kurusu M, et al. A screen of cell-surface molecules identifies leucine-rich repeat proteins as key mediators of synaptic target selection. Neuron. 2008; 59:972–985. [PubMed: 18817735]
13. Shishido E, Takeichi M, Nose A. Drosophila synapse formation: regulation by transmembrane protein with Leu-rich repeats, CAPRICIOUS. Science. 1998; 280:2118–2121. [PubMed: 9641918]
14. Milán M, Weihe U, Pérez L, Cohen SM. The LRR proteins capricious and Tartan mediate cell interactions during DV boundary formation in the Drosophila wing. Cell. 2001; 106:785–794. [PubMed: 11572783]
15. Sakurai KT, Kojima T, Aigaki T, Hayashi S. Differential control of cell affinity required for progression and refinement of cell boundary during Drosophila leg segmentation. Dev Biol. 2007; 309:126–136. [PubMed: 17655839]
16. Mao Y, Kerr M, Freeman M. Modulation of Drosophila retinal epithelial integrity by the adhesion proteins capricious and tartan. PLoS ONE. 2008; 3:e1827. [PubMed: 18350163]
17. Krause C, Wolf C, Hemphälä J, Samakovlis C, Schuh R. Distinct functions of the leucine-rich repeat transmembrane proteins capricious and tartan in the Drosophila tracheal morphogenesis. Dev Biol. 2006; 296:253–264. [PubMed: 16764850]
18. Shinza-Kameda M, Takasu E, Sakurai K, Hayashi S, Nose A. Regulation of layer-specific targeting by reciprocal expression of a cell adhesion molecule, capricious. Neuron. 2006; 49:205–213. [PubMed: 16423695]
19. Wagh DA, et al. Bruchpilot, a protein with homology to ELKS/CAST, is required for structural integrity and function of synaptic active zones in Drosophila. Neuron. 2006; 49:833–844. [PubMed: 16543132]
20. Jefferis GS, et al. Comprehensive maps of Drosophila higher olfactory centers: spatially segregated fruit and pheromone representation. Cell. 2007; 128:1187–1203. [PubMed: 17382886]
21. Wong AM, Wang JW, Axel R. Spatial representation of the glomerular map in the Drosophila protocerebrum. Cell. 2002; 109:229–241. [PubMed: 12007409]
22. Marin EC, Jefferis GS, Komiyama T, Zhu H, Luo L. Representation of the glomerular olfactory map in the Drosophila brain. Cell. 2002; 109:243–255. [PubMed: 12007410]
23. Kohsaka H, Nose A. Target recognition at the tips of postsynaptic filopodia: accumulation and function of Capricious. Development. 2009; 136:1127–1135. [PubMed: 19270171]
24. Sweeney LB, et al. Temporal target restriction of olfactory receptor neurons by Semaphorin-1a/PlexinA-mediated axon-axon interactions. Neuron. 2007; 53:185–200. [PubMed: 17224402]
25. Chang Z, et al. Molecular and genetic characterization of the Drosophila tartan gene. Dev Biol. 1993; 160:315–332. [PubMed: 8253267]
26. Milán M, Pérez L, Cohen SM. Boundary formation in the Drosophila wing: functional dissection of Capricious and Tartan. Dev Dyn. 2005; 233:804–810. [PubMed: 15830355]

27. McLaughlin T, O'Leary DD. Molecular gradients and development of retinotopic maps. Annu Rev Neurosci. 2005; 28:327–355. [PubMed: 16022599]
28. Imai T, Suzuki M, Sakano H. Odorant receptor-derived cAMP signals direct axonal targeting. Science. 2006; 314:657–661. [PubMed: 16990513]
29. Walz A, Rodriguez I, Mombaerts P. Aberrant sensory innervation of the olfactory bulb in neuropilin-2 mutant mice. J Neurosci. 2002; 22:4025–4035. [PubMed: 12019322]
30. Taniguchi M, et al. Distorted odor maps in the olfactory bulb of semaphorin 3A-deficient mice. J Neurosci. 2003; 23:1390–1397. [PubMed: 12598627]
31. Schwarting GA, et al. Semaphorin 3A is required for guidance of olfactory axons in mice. J Neurosci. 2000; 20:7691–7697. [PubMed: 11027230]
32. Schwarting GA, Raitcheva D, Crandall JE, Burkhardt C, Püschel AW. Semaphorin 3A-mediated axon guidance regulates convergence and targeting of P2 odorant receptor axons. Eur J Neurosci. 2004; 19:1800–1810. [PubMed: 15078553]
33. Imai T, et al. Pre-target axon sorting establishes the neural map topography. Science. 2009; 325:585–590. [PubMed: 19589963]
34. Cutforth T, et al. Axonal ephrin-As and odorant receptors: coordinate determination of the olfactory sensory map. Cell. 2003; 114:311–322. [PubMed: 12914696]
35. Kaneko-Goto T, Yoshihara S, Miyazaki H, Yoshihara Y. BIG-2 mediates olfactory axon convergence to target glomeruli. Neuron. 2008; 57:834–846. [PubMed: 18367085]
36. Serizawa S, et al. A neuronal identity code for the odorant receptor-specific and activity-dependent axon sorting. Cell. 2006; 127:1057–1069. [PubMed: 17129788]
37. Stocker RF, Heimbeck G, Gendre N, de Belle JS. Neuroblast ablation in Drosophila P[GAL4] lines reveals origins of olfactory interneurons. J Neurobiol. 1997; 32:443–456. [PubMed: 9110257]
38. Couto A, Alenius M, Dickson BJ. Molecular, anatomical, and functional organization of the Drosophila olfactory system. Curr Biol. 2005; 15:1535–1547. [PubMed: 16139208]
39. Fishilevich E, Vosshall LB. Genetic and functional subdivision of the Drosophila antennal lobe. Curr Biol. 2005; 15:1548–1553. [PubMed: 16139209]
40. Komiyama T, Carlson JR, Luo L. Olfactory receptor neuron axon targeting: intrinsic transcriptional control and hierarchical interactions. Nat Neurosci. 2004; 7:819–825. [PubMed: 15247920]
41. Kreher SA, Kwon JY, Carlson JR. The molecular basis of odor coding in the Drosophila larva. Neuron. 2005; 46:445–456. [PubMed: 15882644]
42. Endo K, Aoki T, Yoda Y, Kimura K, Hama C. Notch signal organizes the Drosophila olfactory circuitry by diversifying the sensory neuronal lineages. Nat Neurosci. 2007; 10:153–160. [PubMed: 17220884]
43. Toba G, et al. The gene search system. A method for efficient detection and rapid molecular identification of genes in Drosophila melanogaster. Genetics. 1999; 151:725–737. [PubMed: 9927464]
44. Wu JS, Luo L. A protocol for mosaic analysis with a repressible cell marker (MARCM) in Drosophila. Nature protocols. 2006; 1:2583–2589. [PubMed: 17406512]
45. Lee T, Luo L. Mosaic analysis with a repressible cell marker for studies of gene function in neuronal morphogenesis. Neuron. 1999; 22:451–461. [PubMed: 10197526]
46. Berdnik D, Fan AP, Potter CJ, Luo L. MicroRNA processing pathway regulates olfactory neuron morphogenesis. Curr Biol. 2008; 18:1754–1759. [PubMed: 19013069]
47. Raymond CS, Soriano P. High-efficiency FLP and PhiC31 site-specific recombination in mammalian cells. PLoS ONE. 2007; 2:e162. [PubMed: 17225864]
48. Stockinger P, Kvitsiani D, Rotkopf S, Tirián L, Dickson BJ. Neural circuitry that governs Drosophila male courtship behavior. Cell. 2005; 121:795–807. [PubMed: 15935765]
49. Schuldiner O, et al. piggyBac-Based Mosaic Screen Identifies a Postmitotic Function for Cohesin in Regulating Developmental Axon Pruning. Dev Cell. 2008; 14:227–238. [PubMed: 18267091]
50. Wu JS, Luo L. A protocol for dissecting Drosophila melanogaster brains for live imaging or immunostaining. Nature protocols. 2006; 1:2110–2115. [PubMed: 17487202]

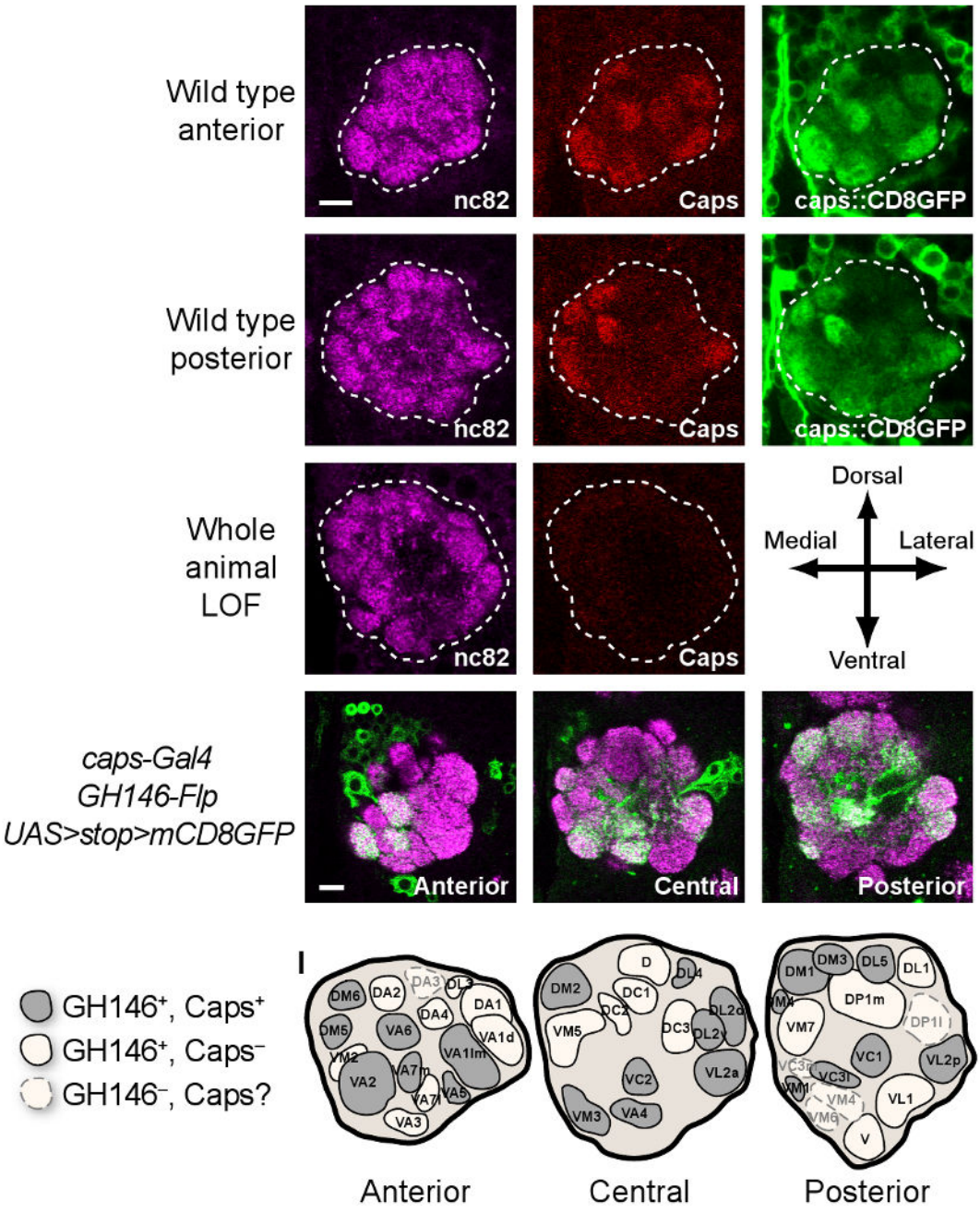


**Figure 1. Caps is differentially expressed in the developing antennal lobe**

(a-h) The developing antennal lobes at 48 hrs APF stained by antibodies against a synaptic marker nc82 (a, d and g), Caps (b, e and h) and *caps-Gal4*-driven mCD8-GFP (c and f). Caps is differentially expressed in the wild-type developing antennal lobe as shown in a single anterior (a-c) and posterior section (d-f) from the same triple-labeled brain. (g-h) Caps staining is absent in $caps^{c28fs}/Df(3L)6118$ trans-heterozygous mutant antennal lobes. (i-k) Expression of a Flp-out GFP reporter *UAS>stop>mCD8GFP* at the intersection of *caps-Gal4* and PN-specific *GH146-Flp* in the adult antennal lobe. Three single sections in

anterior, central, and posterior regions of the antennal lobe are shown. (Magenta: nc82; Green: mCD8GFP)

(l) Schematic representation of the glomerular innervation pattern of *caps-Gal4*-expressing PNs across three different sections of the antennal lobe. Three groups of glomeruli are indicated in the legend to the left. See Fig. S2 for details. Antennal lobes in this and all subsequent images are shown such that dorsal is up and medial is to the left. Scale bars represent 10 μm.

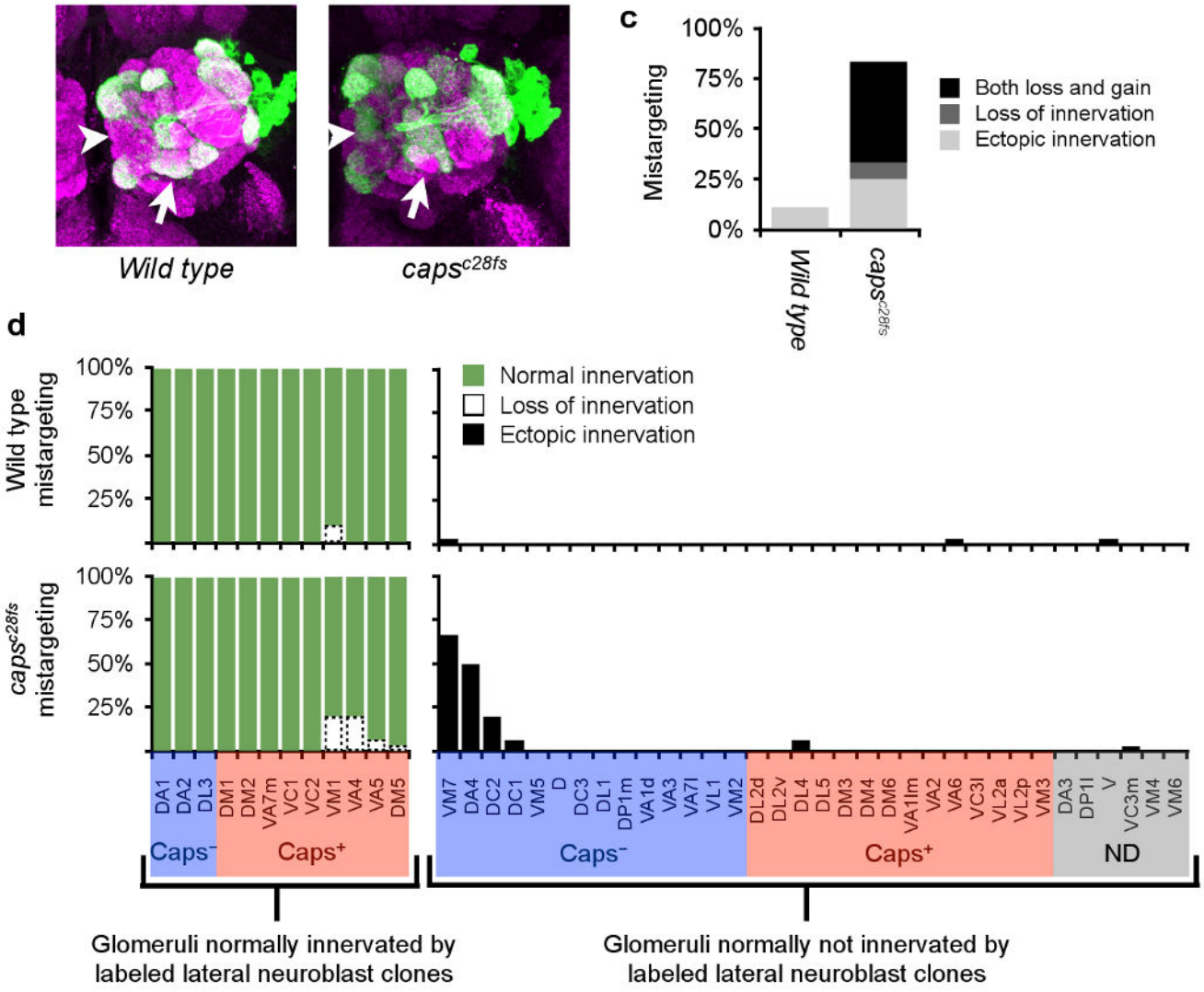


**Figure 2. Dendrite targeting phenotypes of *caps*$^{-/-}$ neuroblast clones**

(a and b) Dendrite targeting of neuroblast MARCM clones of wild-type and *caps*$^{-/-}$ PNs. (a) Wild-type lateral neuroblast clones stereotypically target dendrites to 12 glomeruli. (b) *caps*$^{-/-}$ lateral neuroblast clones exhibit selective dendrite mistargeting: arrowhead indicates the ectopic innervation of VM7 where wild-type PNs do not innervate; arrow indicates the loss of innervation of wild-type glomerular target VA4.

(c) Quantification of dendrite targeting defects in lateral neuroblast MARCM clones of control and *caps* mutant. The Y-axis represents the percentage of the antennal lobes that exhibit mistargeting phenotypes. Light-grey color, dark-grey color, and black color represent the percentages of the antennal lobes: that innervate ectopic glomeruli in addition to the normal glomerular targets, that only exhibit loss of innervation of the normal glomerular targets, and that exhibit both defects, respectively. (Control: n=9; *caps*$^{-/-}$: n=12.)

(d) Glomerular innervation specificity of lateral neuroblast MARCM clones of control and *caps* mutants analyzed in (c). The left 12 columns are the normal glomerular targets of

lateral PNs; green bars: the percentage of antennal lobes in which an individual glomerulus is innervated; white bars: the percentage of antennal lobes in which a normally innervated glomerulus is not innervated. The right 34 columns are glomeruli that are normally not innervated by lateral PNs; black bars: the percentage of antennal lobes in which an ectopic glomerulus is innervated. All glomeruli are color-coded at the bottom based on the expression of Caps in the corresponding PNs as indicated. ND, not determined for Caps expression (*GH146*-negative).

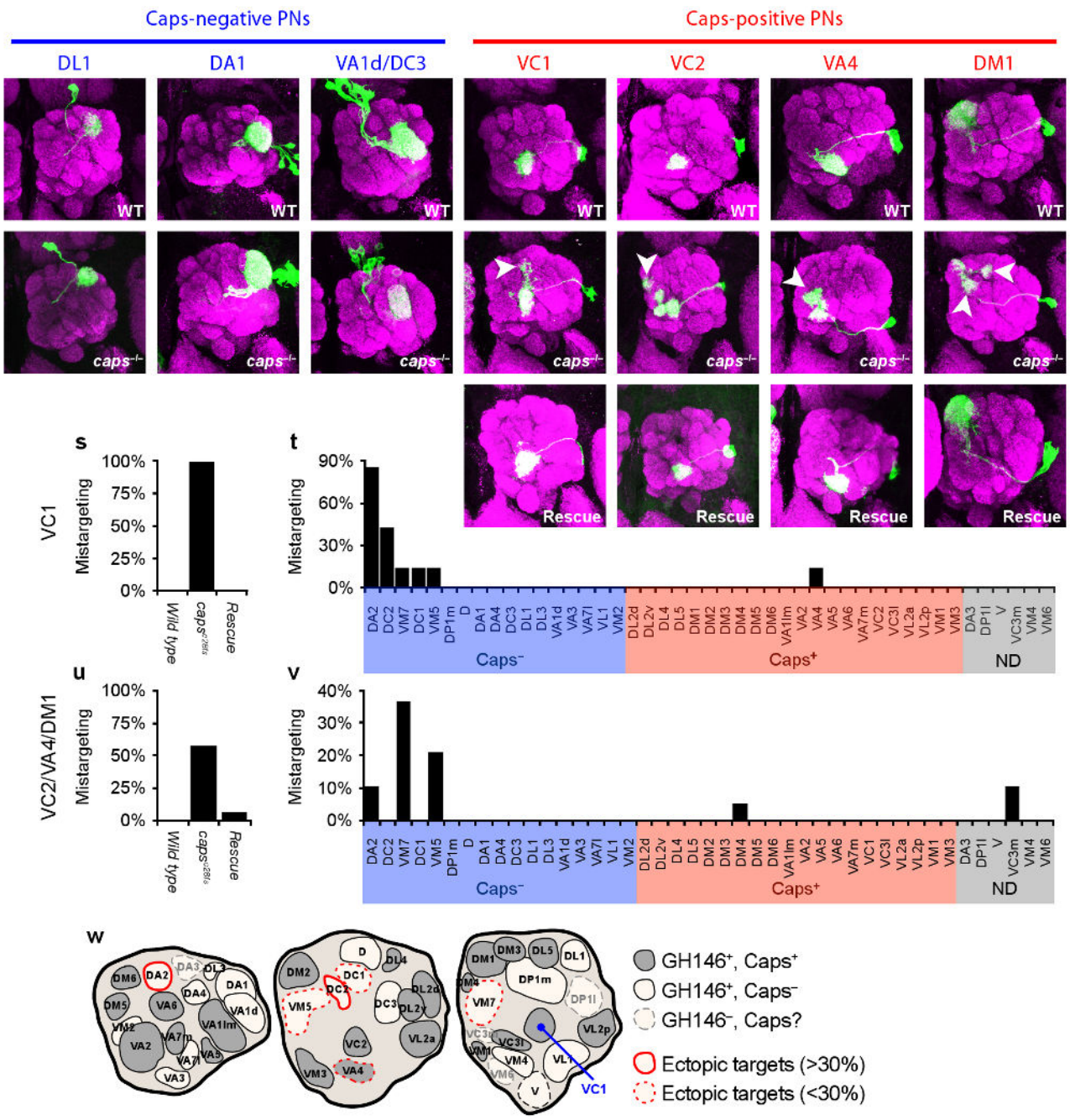


**Figure 3. Cell-autonomous requirement of Caps in Caps-positive PNs for dendrite targeting**

(a-c, h-j) Normal dendrite targeting of *caps*$^{-/-}$ MARCM clones in DL1 single cells (h), DA1 neuroblasts (i) and VA1d/DC3 neuroblasts (j), compared with wild-type (a-c). These PNs are all Caps-negative. n=20 for both wild-type and *caps*$^{-/-}$.

(d-g, k-n) Defective dendrite targeting of VC1, VC2, VA4 and DM1 PNs in single-cell *caps*$^{-/-}$ clones (k-n) compared with wild-type (d-g). These PNs are all Caps-positive. Their identities are determined as described in the Methods.

(o-r) Rescue of dendrite targeting of four Caps-positive PNs by expressing a *UAS-caps* transgene only in the single-cell clones.

(s-v) Quantification (s, u) and glomerular innervation specificity (t, v) of dendrite targeting defects in single-cell clones of control and *caps* mutant analyzed in (d-g, k-r). VC2, VA4 and DM1 were analyzed together (see Methods). (s, u) Y-axes represent the percentage of PNs in particular classes that exhibit dendrite mistargeting phenotypes. (t, v) Each black bar indicates the percentage of antennal lobes in which an ectopic glomerulus is innervated. All glomeruli are color-coded at the bottom as in Fig. 2d. VC1 and VC2/VA4/DM1 classes are omitted in t and v, respectively, as they are the ones from which clones were made. (Wild-type: VC1 n=15, VC2 n=15, VA4 n=15, DM1 n=10; $caps^{-/-}$: VC1 n=7; VC2/VA4/DM1 n=19; Rescue: VC1 n=6, VC2 n=5, VA4 n=6, DM1 n=4).

(w) Schematic representation of the glomerular innervation pattern of individual $caps^{-/-}$ VC1 PNs across three different sections of the antennal lobe. Red glomeruli are the ectopic targets of $caps^{-/-}$ VC1 dendrites.

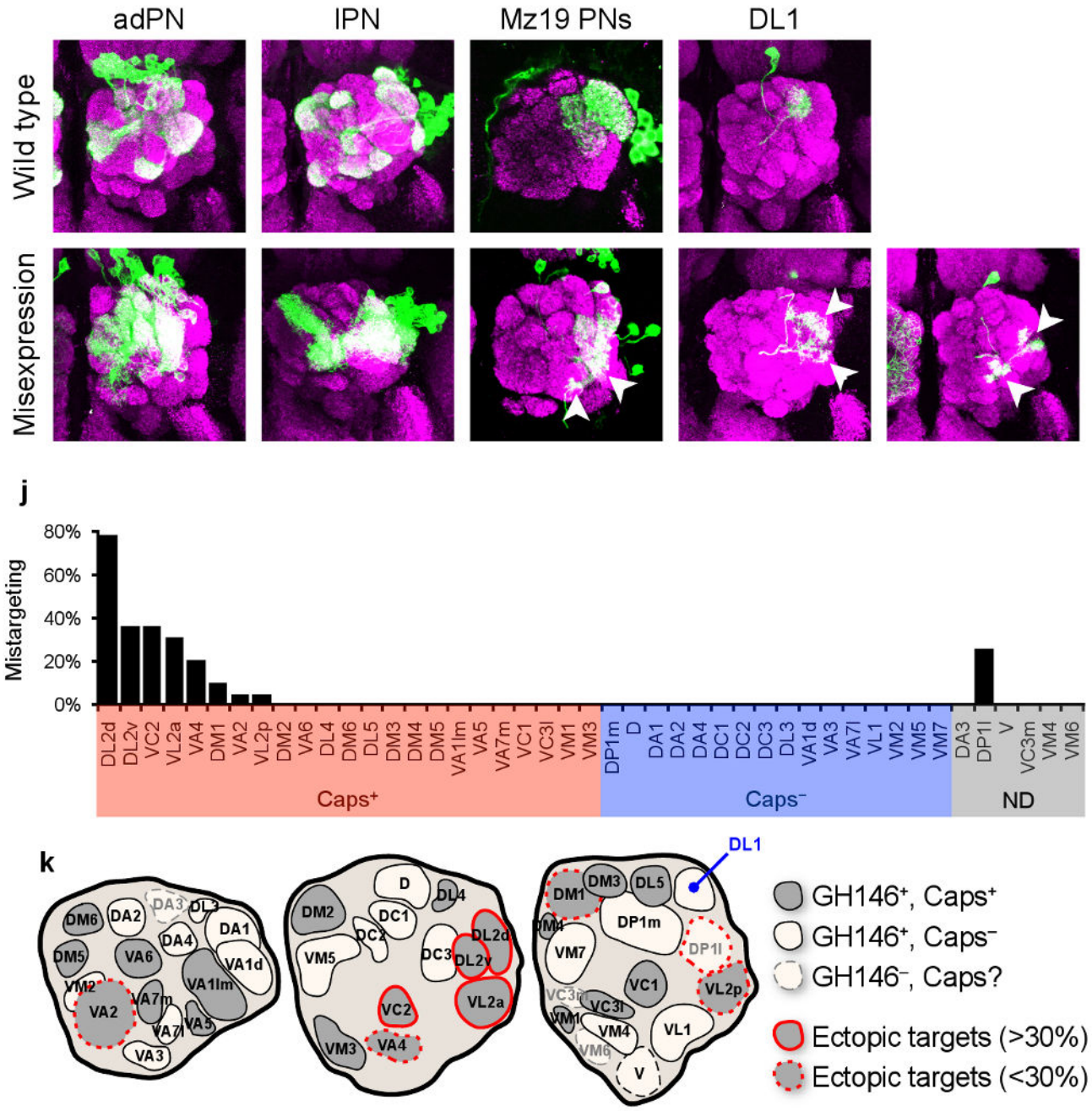


**Figure 4. Dendrite targeting phenotypes of Caps misexpression in Caps-negative PNs**

(a-d) MARCM overexpression of Caps in anterodorsal (b) and lateral (d) neuroblast clones shows severe mistargeting phenotypes, compared to wild type neuroblast clones (a and c). (Control: n=9; Caps misexpression: n=10).

(e-f) Caps misexpression in DA1, DC3 and VA1d PNs using *Mz19*-Gal4 shows strong mistargeting of dendrites to VA1lm and VA4 (arrowheads), both of which are normally innervated by Caps-positive PNs. (Control: n=40; Caps misexpression: n=48).

(g-i) Misexpression of Caps in single DL1 PNs using *GH146*-Gal4 causes mistargeting of dendrites to ectopic glomeruli (arrowheads in h-i).

(j) Quantification of glomerular innervation pattern of individual DL1 PNs misexpressing Caps. Each black bar indicates the percentage of antennal lobes in which an ectopic glomerulus is innervated. All glomeruli are color-coded at the bottom as in Fig. 2d. (Control: n=20; Caps misexpression: n=19).

(k) Schematic representation of the glomerular innervation pattern of individual Caps-misexpressing DL1 PNs across three different sections of the antennal lobe. Red glomeruli: ectopic targets of DL1 dendrites misexpressing Caps.

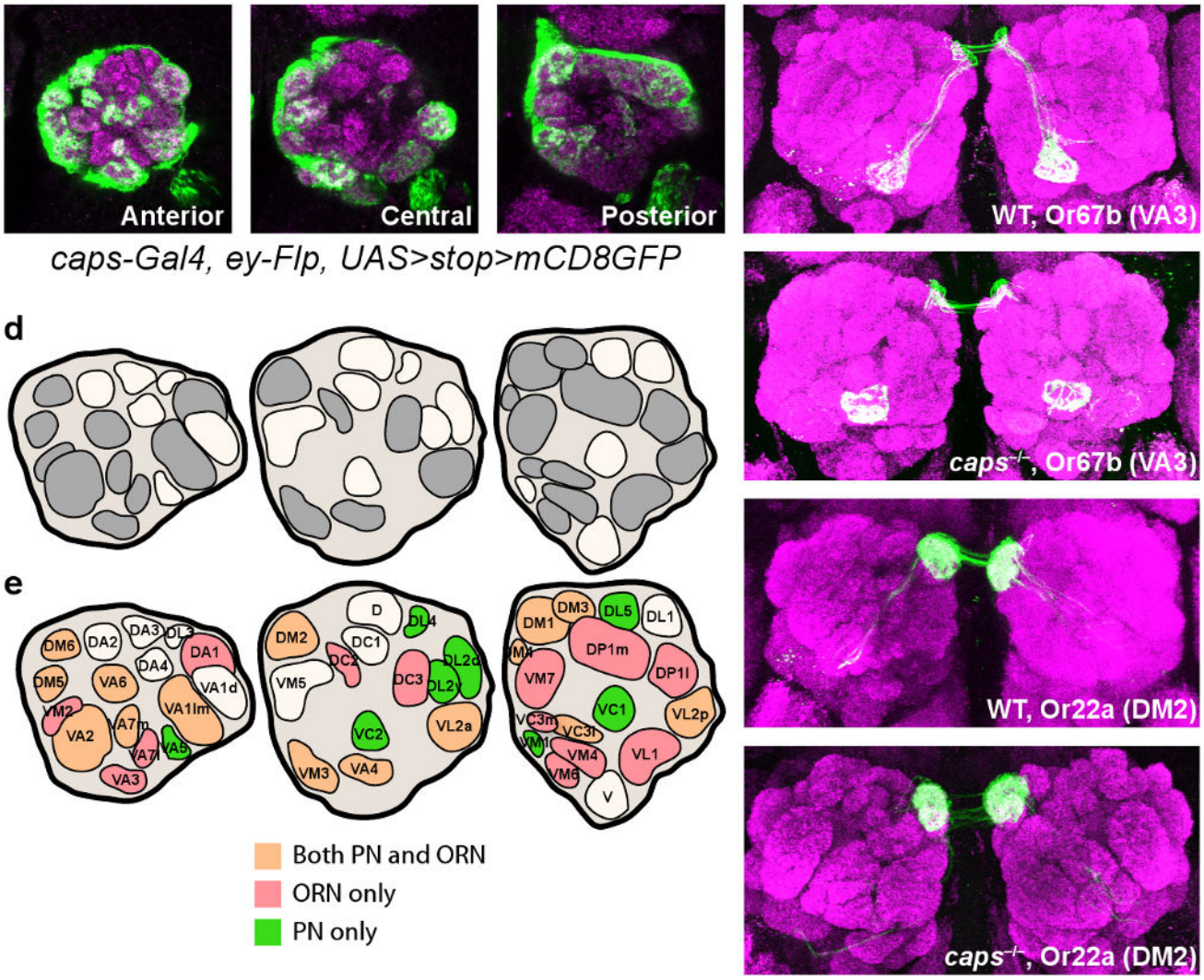


**Figure 5. *caps* is not required in ORNs for their axon targeting**

(a-c) Expression of an intersectional reporter *UAS>stop>mCD8GFP* for *caps-Gal4* and *ey-Flp*. (*ey-Flp* is expressed in ORN precursors but not PNs or their precursors). Magenta: nc82; Green: mCD8GFP.

(d) Schematic representation of the glomerular innervation pattern of *caps-Gal4* expressing ORNs across three different sections of the antennal lobe. Gray glomeruli: targets of *caps-Gal4* positive ORNs; white glomeruli: targets of *caps-Gal4* negative ORNs.

(e) Schematic comparison of the innervation pattern of Caps-positive PNs and ORNs. See also Fig. S2.

(f-i) Axon targeting of ORNs in the antennal lobe is not affected in $caps^{-/-}$ ORNs. Or67b ORNs innervating VA3 and Or22a ORNs innervating DM2 are shown. In these experiments, only $caps^{-/-}$ axons of a particular class of ORNs are visualized by the Gal4 lines, whereas all the cells in the central brain, including all PNs, are heterozygous because *ey*-Flp restricts recombination in the olfactory system to the peripheral organs.

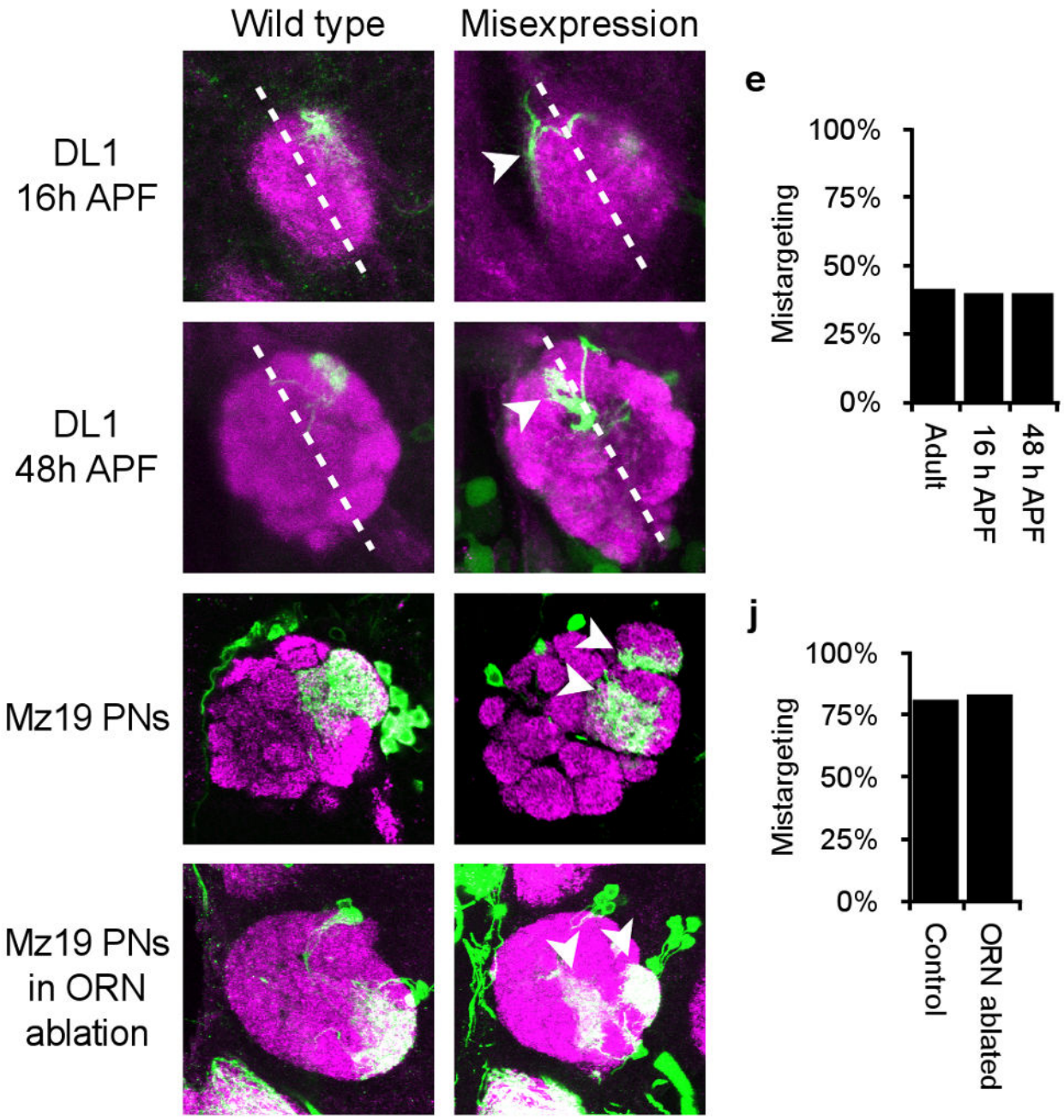


**Figure 6. Caps-mediated PN dendrite targeting is independent of ORNs**

(a-d) Mistargeting of DL1 PN dendrites caused by Caps misexpression is observed at early developmental time points. Dotted lines bisect the antennal lobe into dorsolateral and ventromedial parts. Arrowheads in (b) and (d) point to DL1 dendrites that cross the dotted line and invade the ventromedial part of the antennal lobe.

(e) Quantification of mistargeting across the dorsomedial-ventrolateral midline of the antennal lobe (dotted lines in a-d) at different developmental stages. Adult: n=12; 16 hrs APF: n=10; 48 hrs APF: n=5.

(f-j) Caps misexpression by *Mz19*-Gal4 causes a segregation of dendritic field as a consequence of dendrite mistargeting to VA1lm and VA4 (arrowheads in g), compared to continual dendritic field from control *Mz19*-Gal4 labeled PNs (f). Caps misexpression by *Mz19*-Gal4 in ORN-ablated animals causes dendrite segregation (i) compared with control *Mz19* PNs in ORN-ablated animals which forms a continual field (h). (j) Quantification of the dendrite segregation phenotypes caused by *Mz19*-Gal4 misexpression of Caps, with and without ORN ablation. Caps misexpression without ORN ablation: n=48; Caps misexpression with ORN ablation: n=18.

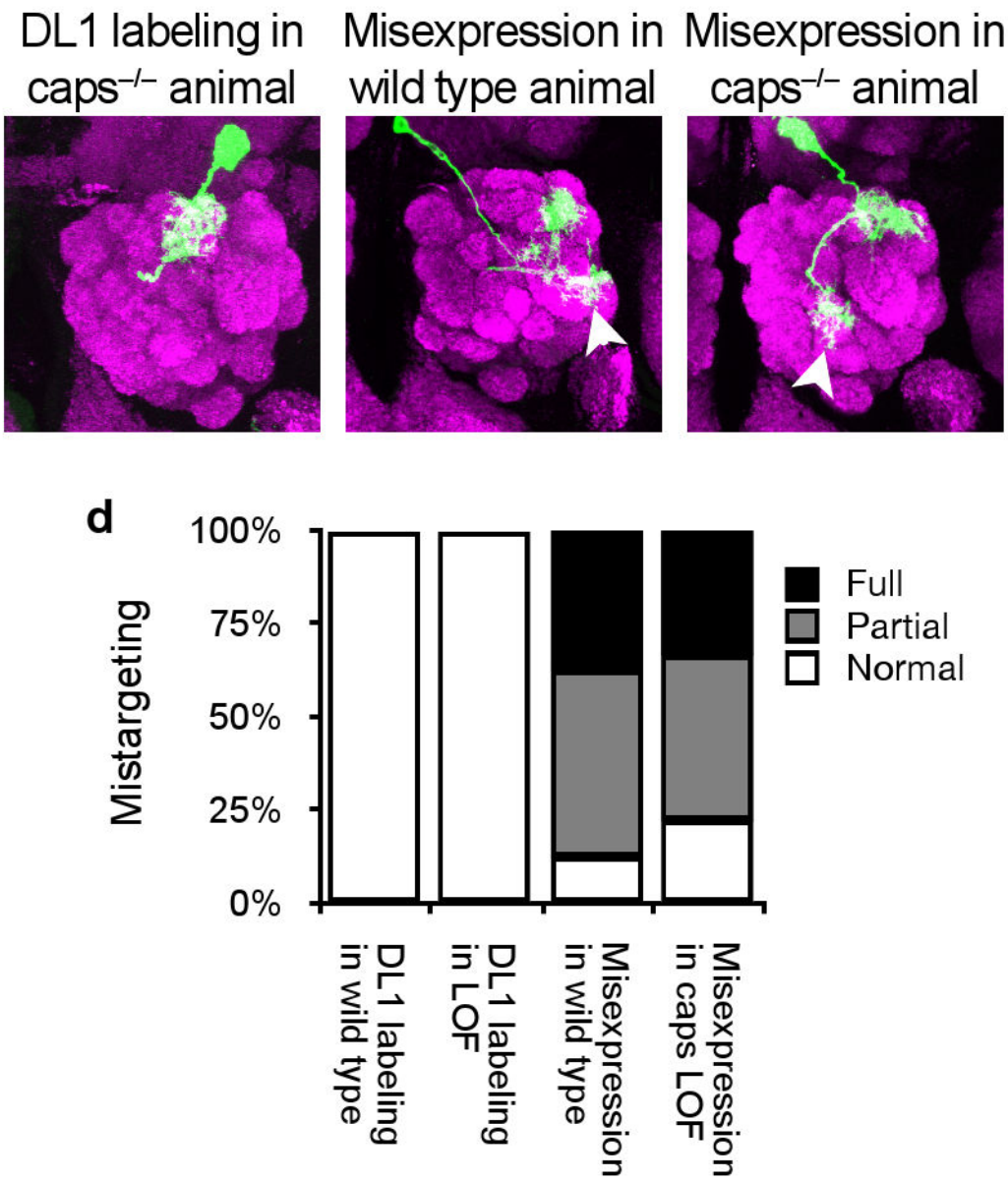


**Figure 7. Caps does not mediate homophilic interactions for PN dendrite targeting**

(a) Normal dendrite targeting of a single DL1 PN in a *caps* whole animal mutant (*caps*$^{c28fs}$/*Df(3L)6118*).

(b-c) Dendrite mistargeting of a single DL1 PN misexpressing Caps in an otherwise wild-type background (b) or an otherwise *caps*$^{c28fs}$/*Df(3L)6118* mutant background (c).

(d) Quantification of DL1 targeting defects for genotypes in a-c. (DL1 labeling in wild-type background: n=20; DL1 labeling in trans-heterozygous mutant background: n=20; Caps misexpression in a otherwise wild-type background: n=8; Caps misexpression in a otherwise trans-heterozygous mutant background: n=9). Grey bars represent the percentage of partial mistargeting events in which PN dendrites still partially innervate DL1 and black bars represent the percentage of full mistargeting events in which no dendrites innervate DL1.

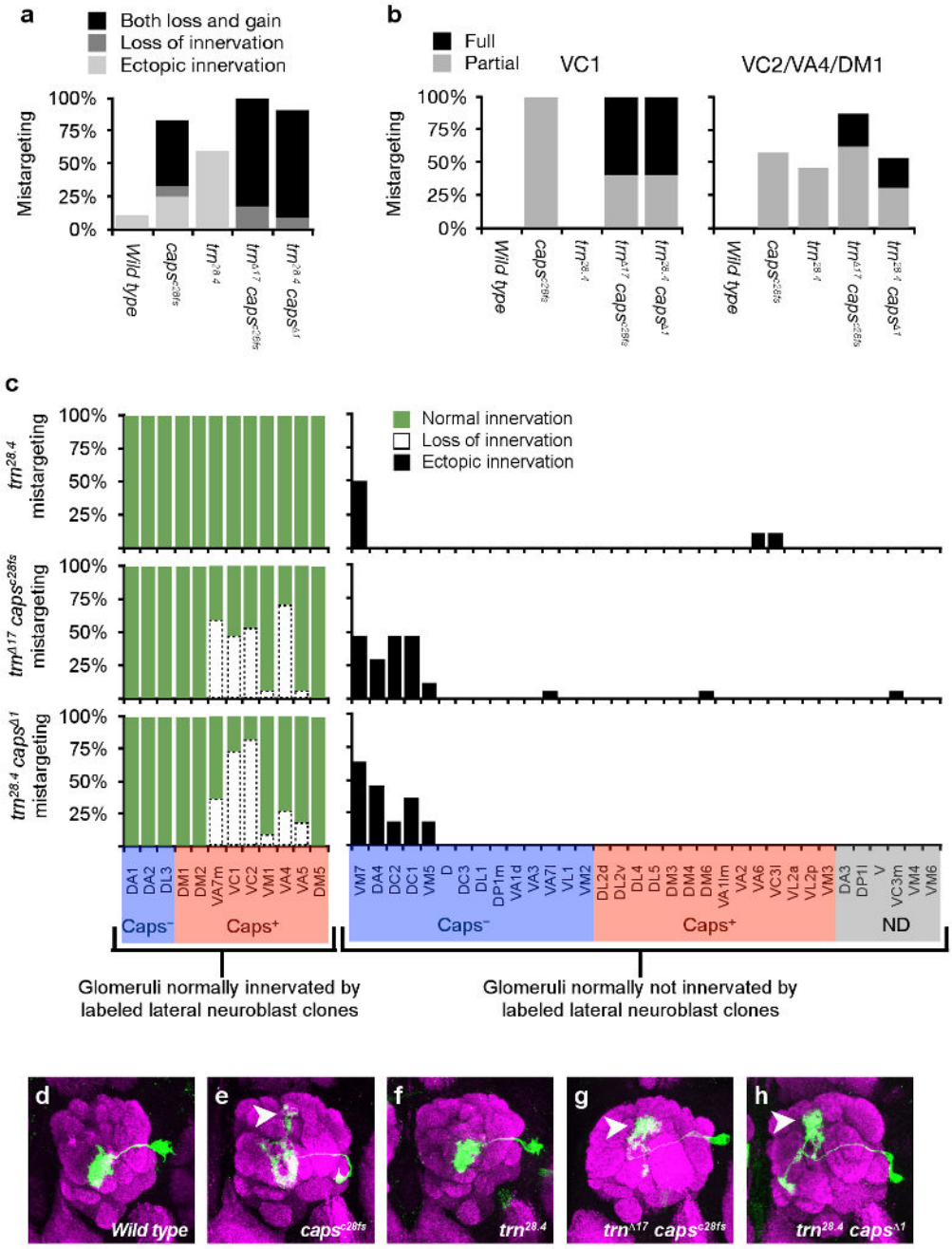


**Figure 8. *trn* enhances *caps* phenotypes in PN dendrite targeting**

(a) Quantification of dendrite targeting defects in lateral neuroblast MARCM clones of control, single, and double mutants of *caps* and *trn* as indicated. The Y-axis and the colored bars are represented as described in Fig. 2c. (Wild-type: n=31; $caps^{c28fs}$ *FRT2A*: n=30; $trn^{28.4}$ *FRT2A*: n=18; $trn^{\Delta 17}$ $caps^{c28fs}$ *FRT2A*: n=17; $trn^{28.4}$ $caps^{\Delta 1}$ *FRT80B*: n=11)

(b) Quantification of dendrite targeting defects in single-cell MARCM clones of control, single, and double mutants of *caps* and *trn* as indicated. The Y-axis and the bars are represented as described in Fig. 7d. (For VC1, wild-type: n=20; $caps^{c28fs}$ *FRT2A*: n=7;

*trn*$^{28.4}$ *FRT2A*: n=5; *trn*$^{\Delta 17}$ *caps*$^{c28fs}$ *FRT2A*: n=5; *trn*$^{28.4}$ *caps*$^{\Delta 1}$ *FRT80B*: n=5. For VC2/VA4/DM1, wild-type: n=30, *caps*$^{c28fs}$ *FRT2A*: n=19, *trn*$^{28.4}$ *FRT2A*: n=13, *trn*$^{\Delta 17}$ *caps*$^{c28fs}$ *FRT2A*: n=16, *trn*$^{28.4}$ *caps*$^{\Delta 1}$ *FRT80B*: n=13).

(c) Glomerular innervation specificity of lateral neuroblast MARCM clones of *trn* single mutant and *caps, trn* double mutants analyzed in (a). The Y-axis and the colored bars are represented as described in Fig. 2d.

(d-h) Dendrite targeting of single-cell VC1 MARCM clones of control, single, and double mutants of *caps* and *trn* as indicated. Arrowheads indicate the ectopic innervation of DA2 where wild-type VC1 PNs do not innervate.